12th International Workshop on Wave Hindcasting and Forecasting, Kohala Coast, Hawai'i, HI, 2011.

THE IMPACT OF NONLINEAR INTERACTION PARAMETERIZATIONS ON PRACTICAL WIND WAVE MODELS [1]

Hendrik L. Tolman[2]

NOAA / National Centers for Environmental Prediction
Environmental Modeling Center
Marine Modeling and Analysis Branch
Camp Springs, Maryland, USA

1 INTRODUCTION

Third-generation wind wave models are models where all physical processes governing wave growth and decay are explicitly parametrized, allowing for a direct integration in time of all sources and sinks of wave energy without the need for prescribed spectral shapes. The critical element in such models is the computation of nonlinear interactions between so-called quadruplets of four wave components. These interactions have two features that make them essential for evaluating wind wave growth. First, they are thought to be the lowest order process capable of shifting wave energy to lower frequencies, and hence lengthening the waves during growth. Secondly, they are stabilizing spectral shapes for frequencies above the spectral peak frequency. The practical implications of these nonlinear interactions were solidly established in the JONSWAP experiment (Hasselmann et al., 1973). Reviews of the interactions and their impact can be found in, for instance, Masuda (1980), Phillips (1981), Young and Van Vledder (1993), Komen et al. (1994), Van Vledder (2006), or WISE Group (2007). In the present study, only selected references will be used as relevant , but not intended to give a complete overview of the body of work available on this subject.

The full evaluation of the nonlinear interactions requires the integration of a six-dimensional Boltzmann integral, including a complex interaction coefficient with moving singularities. One way of evaluating these 'exact' interactions is the so-called Webb-Resio-Tracy method (Webb, 1978; Tracy and Resio, 1982; Resio and Perrie, 1991), as implemented in the portable software package of Van Vledder (2002, 2006)[3]. Such packages make it feasible to evaluate the exact interactions in research models, but the resulting algorithms require several orders of magnitude more computational time than is economically feasible for practical (operational) third-generation wind wave models.

Operational third-generation wind wave models became feasible with the development of the Discrete Interaction Approximation (DIA, Hasselmann et al., 1985). This approximation requires a similar computational effort as all other parts of a typical wave model combined. The development of the DIA made operational third-generation wave models like WAM (WAMDIG, 1988), WAVEWATCH (Tolman, 1991), and SWAN (Booij et al., 1999) feasible. However, from its inception, the DIA was recognized as having limited accuracy, and much effort has been expended in the ensuing decades to provide a more accurate yet economical parameterization of the nonlinear interactions. This effort has lead to more economical near-exact approaches, and more accurate reduced approaches (cf. the DIA). For semi-operational wave model applications the SRIAM method (e.g., Komatsu, 1996; Tamura et al., 2008) and the Generalized Multiple DIA (e.g., Tolman, 2009a, 2010b) have a proven record. Other methods like the Two-Scale Approximation (TSA, Resio and Perrie, 2008; Perrie and Resio, 2009) and Neural Network approaches (e.g., Tolman and Krasnopolsky, 2004; Tolman, 2009a) show promise.

[1] MMAB contribution Nr. 293
[2] E-mail:Hendrik.Tolman@NOAA.gov
[3] Model version 5.04 used here

Most of the above studies address the impact of improved interactions by showing reduced errors in interactions for test spectra, and in some case by showing improved model integration behavior in idealized test cases. Only for the GMD, explicit real-world test cases are considered to address the impact of the choice of interaction parameterization on wind wave model behavior (Tolman, 2010b). The present manuscript presents a further refined version of the real-world test cases of the latter report. The tests consist of a synthetic hurricane run (Section 2), and a real-world storm case on Lake Michigan (Section 3). Objective accuracy estimates and relative model run time estimates are presented in Section 4, and conclusions are presented in Section 5.

All computations in the present study are performed with the WAVEWATCH III® wave modeling framework (Tolman et al., 2002; Tolman, 2009b, henceforth denoted ad WW3). Used here is version 3.15, which augments the publicly released version 3.14 with a fully optimized GMD code. Benchmark results for each model application are obtained using the default model setup, replacing the DIA with the 'exact' WRT package mentioned above. From such a benchmark reference run, a set of spectra are saved. Similar runs are performed with interaction approximations to be tested, saving the equivalent model spectra. From the two sets of spectra a set of objective error measures are computed, including mean wave parameters, one-dimensional spectral parameters, and full two-dimensional spectral parameters (see Tolman, 2010b, for details). For details on model equations including the GMD, reference is made to the above quoted papers. Model (interaction) configurations used in this study are gathered in Table 1.

Table 1: Nonlinear interaction configurations used in this study. Note that WAM implies nonlinear interaction configuration, not other physics from WAM model.

ID	Description
WAM	GMD with DIA config. from WAM
WW3	GMD with DIA config. from WW3
G11d	GMD with optimized DIA config.
G13d	GMD with 3 DIA quadruplets.
G35d	GMD with 5 quadruplets that are fully configurable.
WRT	Exact interactions (baseline)

Several additional consideration apply to this study. First, the GMD is used as a proxy for a set of increasingly complex and accurate nonlinear interaction parameterizations. This is done because other parameterizations, like the SRIAM and TSA, are not (yet) available in WW3. Once such parameterizations become available in WW3, they can easily be added to the model comparison, using the optimization and validation package designed for the GMD as presented in Tolman (2010a). The latter package is intended to be distributed with the next public release of WW3, and includes the two real-world test considered here.

Second, the default source term options in WW3 have been developed (tuned) to operate with the DIA, and hence are not expected to be fully optimized when used in the baseline WRT computation. It is therefore sensible to compare model results obtained with other nonlinear parameterizations to the baseline WRT results, but it is not sensible to compare the various model results to observations which are available for the Lake Michigan case.

Finally, as noted in Tolman (2010b) computations with the WRT are sensitive to the discrete spectral range used in the wave model. For the hurricane test presented in the latter report the range was insufficient, which was remedied for the Lake Michigan case. For the present study, the hurricane test have been recomputed with an expanded discrete frequency range, which accounts for differences in hurricane results presented here when compared to the results of Tolman (2010b).

2 HURRICANE CASE

The synthetic hurricane considered here is taken from one of the test cases distributed with WW3. The hurricane winds are described with a Rankin vortex with a maximum wind speed of 45 ms^{-1} and a radius of maximum wind of 50 km. The hurricane (and the computational grids) move to the right (east) with a speed of 5 ms^{-1}. Three telescoping grids with resolutions of 50, 15 and 5 km are used. All grids are centered on the eye of the hurricane. Computations start with an ocean at rest, and continue for 24 h, at which time the spectra at 33 locations are saved for model intercomparisons (see Fig. 1). The maximum wave height at the end of the computation exceed 12 m and occur at the south-east of the eye, in the area where the so-called 'dynamic fetch' occurs (see Fig. 1).

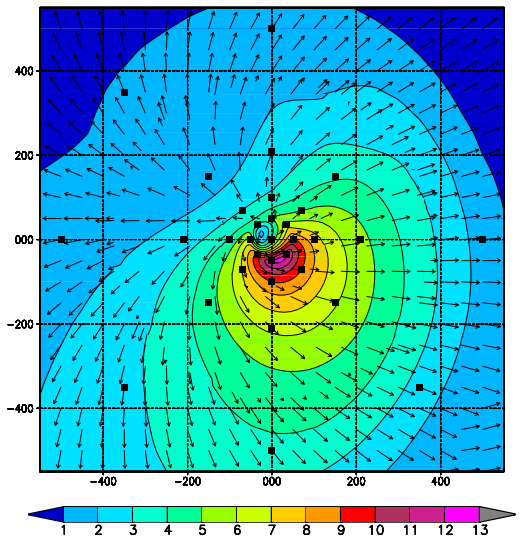

Fig. 1: Significant wave heights H_s in m for the reference WRT model run at the end of the computation. Symbols identify locations where test spectra are saved.

The GMD in the traditional DIA configuration results in surprisingly large errors in wave heights ($>$ 1 m, error defined as differences between approximate and exact interactions). This is illustrated in Fig. 2a with the differences between the WW3 configuration and the reference results of Fig. 1. The largest errors occur away from the largest wave heights, and correspond to local relative wave height error of over 20% (Figure no presented here). The WW3 results are representative in magnitude with those of other DIA configurations (WAM, G11d), although error patterns may differ in details. For all DIA configurations positive wave height errors occur to the north, whereas negative errors occur to the south and east. Considering three representative quadruplets while using the quadruplet configuration of the DIA (G13d, Fig. 2b) reduces wave height errors to be generally less than 0.5 m, except for small areas near the eye of the storm. Considering five representative quadruplets while using arbitrarily configurable quadruplets (G35d, Fig. 2c) virtually removes wave height errors with error exceeding 0.2 m only in a small area near the maximum wave height. For practical hurricane wave forecasting, model errors still appear dominated by errors in the wind forecasts, and validation is hampered by the sparsity of observations (e.g., Tolman et al., 2005). However, systematic differences in wave heights per quadrant of up to 20% should be notable in operational forecasting.

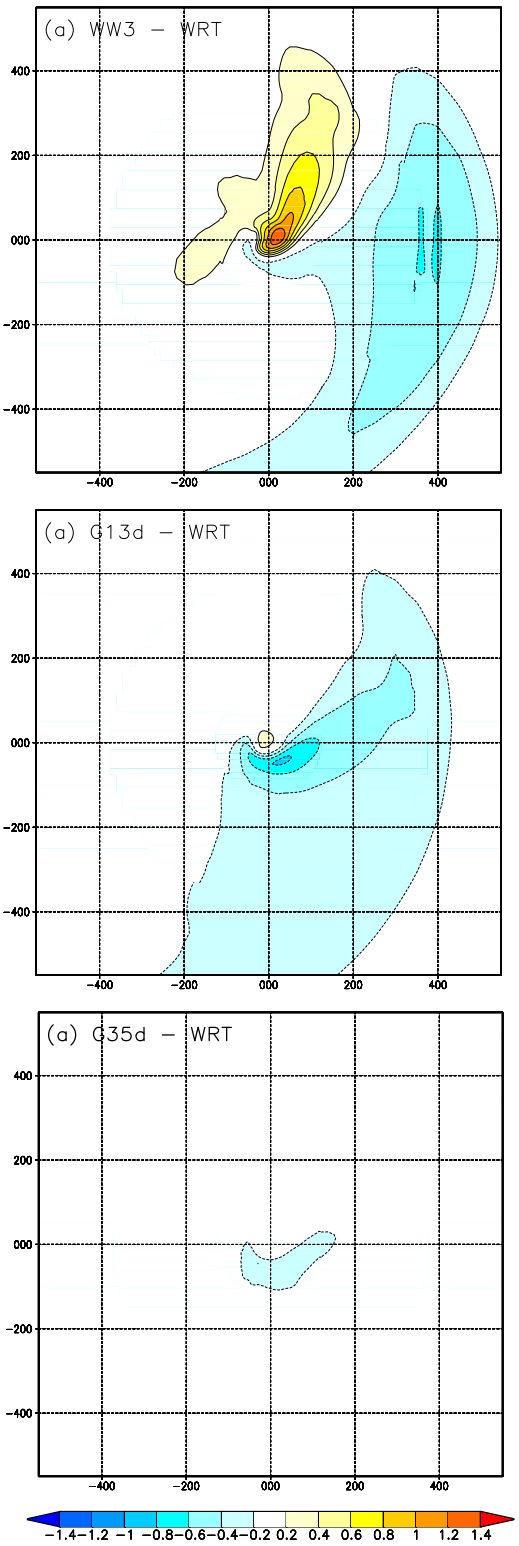

Fig. 2: Significant wave height differences in m with reference run for the hurricane for various interaction approximations from Table 1. (a) WW3. (b) G13d. (c) G35d.

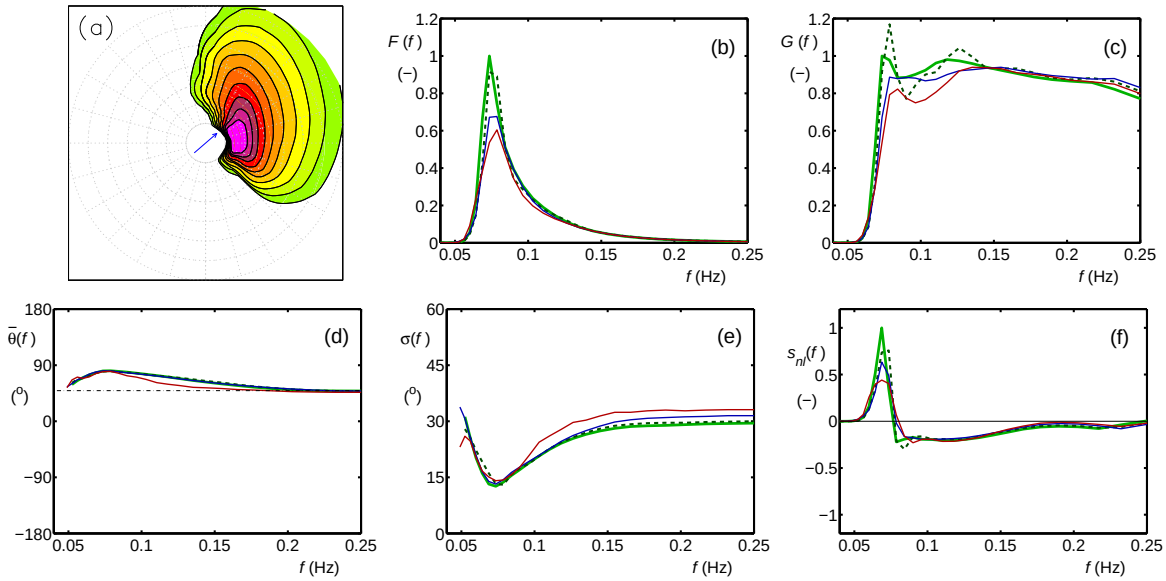

Fig. 3: Spectral behavior of various nonlinear approaches for output point 35 km south and 35 km east of eye of hurricane. (a) Two-dimensional spectrum. (b) One-dimensional spectrum. (c) Steepness spectrum.(d) Mean spectral direction. (e) Directional spread. (f) Interactions. Green line: exact (WRT) solution. Dashed green line: G35d. Blue line: G13d. Red line: G11d. Dashed black line in (d) represents wind direction.

The hurricane test case includes a wide variety of wave conditions, including dominant (sheared) wind seas, dominant swells, and mixed seas. Figure 3 shows spectral results for a slightly sheared wind sea, near the location of the maximum wave height. Results for the various nonlinear approaches at this location are similar to those obtained for the idealized test cases in Tolman (2010b); In the energy spectrum (Fig. 3b) the DIA equivalent approach (G11d, red line) severely underestimates the spectral peak (WRT, green line), the expanded DIA (G13d, blue line) reduces this error and the most complex GMD considered here (G35d, dashed green line) removes most of the error. Similar behavior is found for the interactions (Fig. 3f), and the DIA equivalent approach overestimates the directional spread above the spectral peak frequency (Fig. 3e).

Figure 4 shows spectral results for a swell traveling ahead of the hurricane in the northeastern quadrant. Note that the optimization of the GMD focuses on wind seas, and not on swell, with the implicit assumption that accurate swell predictions require accurate predictions of the wind seas from which they originate. The testing, however, does not explicitly enforce accurate interactions for resulting swells. For the spectrum and steepness spectrum (Figs. 4b,c) the G13d and G35d approaches show a moderate but expected improvement compared to the DIA (G11d) approach. The interaction signature of the swell (Fig. 4f) for frequencies below 0.1 Hz is surprisingly accurate for the G13d approach (blue line), and qualitatively accurate for the G35d approach (dashed green line).

Finally, Fig. 5 shows a case with a developing bimodal sea. The full spectrum (Fig. 5a) shows a wind sea developing under a nearly straight angle with a swell. In the one-dimensional spectrum and steepness spectra (Figs. 5b,c), the two wave fields can also be identified, albeit not as clearly as in the full spectrum. Improvements with increasing complexity of the interaction approximation again are clear. Particularly impressive is the resulting interaction from the G35d approach (dashed green line in Fig. 5f), which follows the non-conventional signature of the exact interactions (solid green line) with a high degree of accuracy. The G13d approach is also an impressive improvement over the DIA, with getting patterns reproduced accurately, but with some amplitude errors compared to the G35d approach.

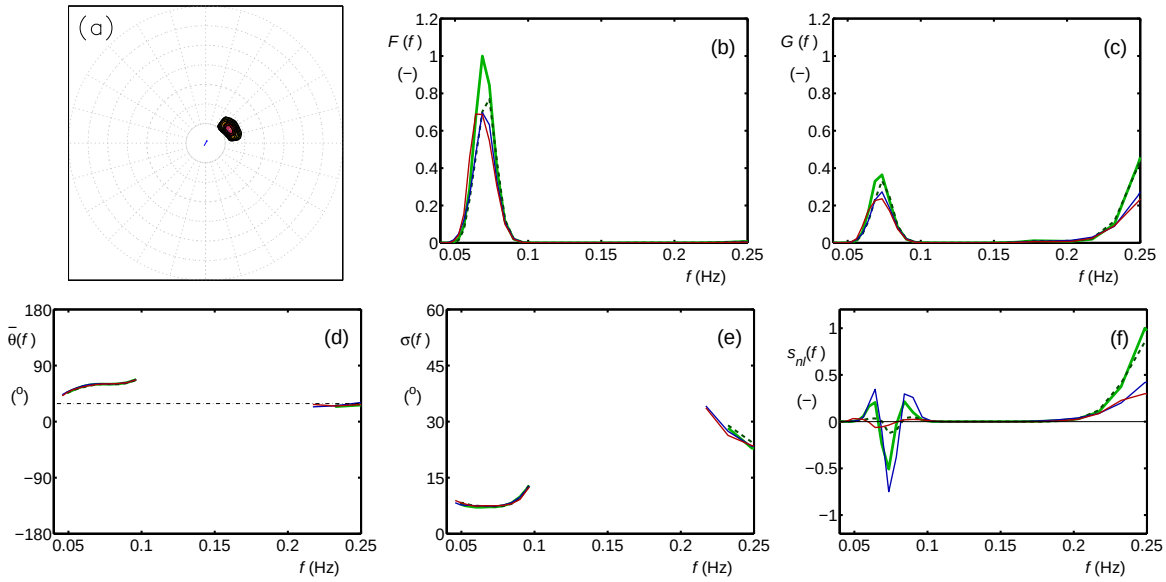

Fig. 4 : Like Fig. 3 for output point 350 km north and 350 km east of eye of hurricane.

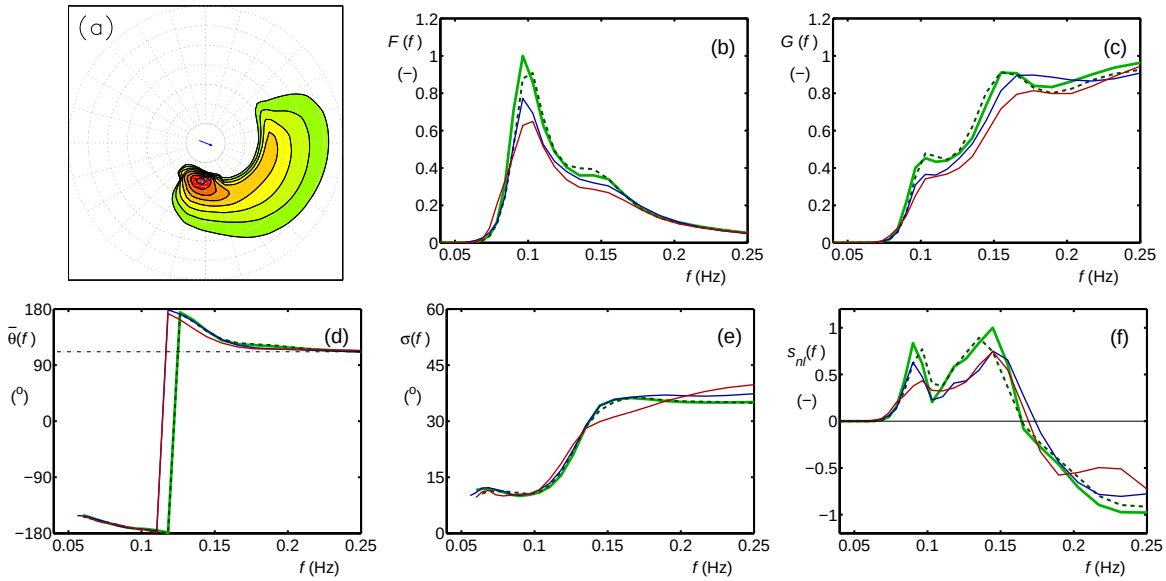

Fig. 5 : Like Fig. 3 for output point 350 km south and 350 km west of eye of hurricane.

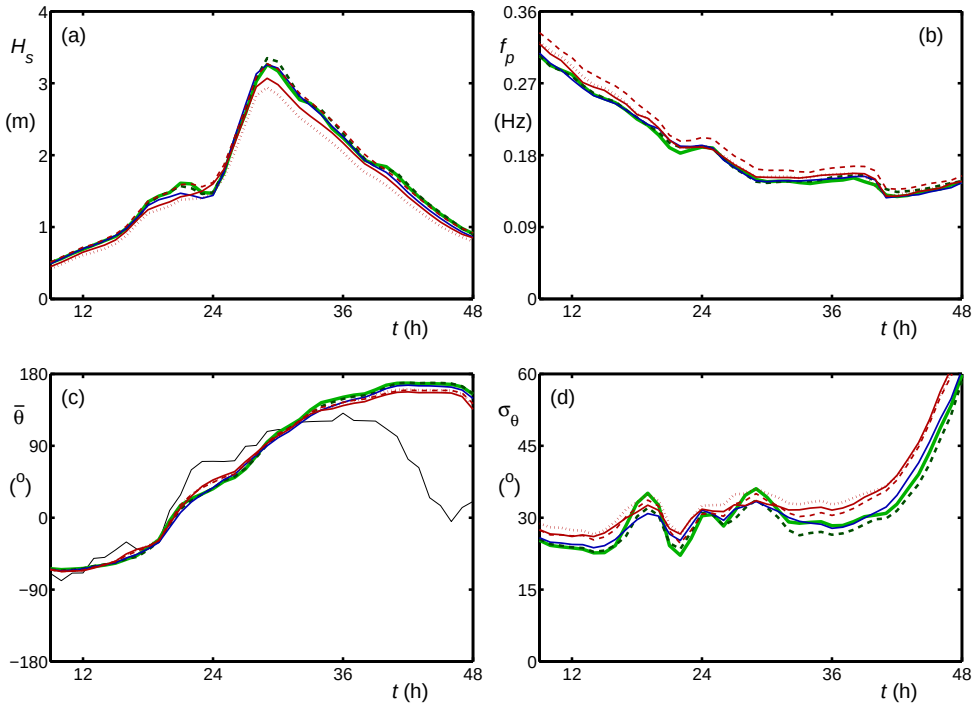

Fig. 7: Evolution in time of a) significant wave height, b) peak frequency , c) mean direction, and d) directional spread at location 45007 for the Lake Michigan test case. Time in h from Oct. 6, 2009, 00z, saving data starting at 09z. Green: WRT. Dashed green: G35d. Blue: G13d. Red: G13d. Red dashed : WW3. Red dotted: WAM. Solid black line in panel c represents wind direction.

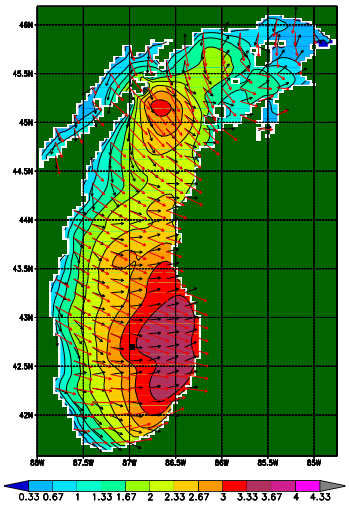

Fig. 6: Significant wave heights H_s in m for the reference WRT model run for Lake Michigan at Oct. 7 05z. The symbol at the south side of the lake identifies the location of buoy 45007 where hourly test spectra are saved. Black and red vectors are wave and wind directions, respectively.

3 LAKE MICHIGAN

The second realistic test considers a storm on Lake Michigan on Oct. 6-7, 2009. The model grid is taken from NCEP's operational Great Lakes wave models, and winds consist of analyses performed by The Great Lakes Environmental Research Laboratory (GLERL). The peak of the storm in the southern part of the lake occurs around 05z on October 7 with wave conditions as shown in Fig. 6. Hourly spectra are saved for the location of buoy 45007 (see Fig. 6). The model is started without waves, and the results for the first nine hours of October 6 are discarded as a spin-up for the model, resulting in 40 spectra for validation.

For the Lake Michigan test, the differences between the models with the various interaction approximations are smaller than for the hurricane. This is illustrated with the time evolution of mean wave parameters at the location of buoy 45007 in Fig. 7, showing the wave height, spectral peak frequency, mean wave direction and mean directional spread for all model configurations of Table 1.

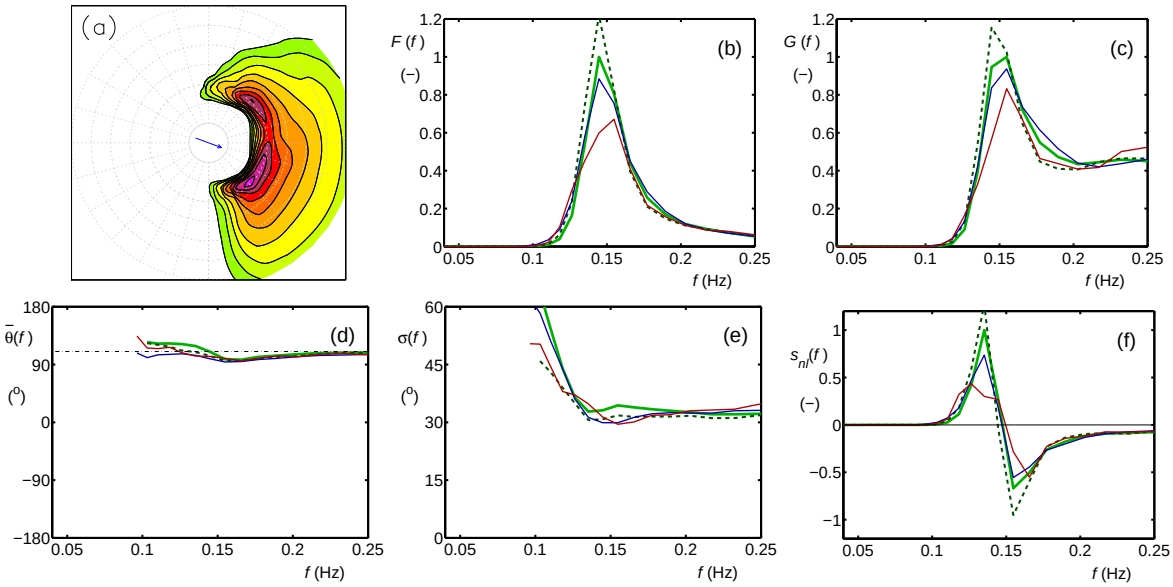

Fig. 8 : Like Fig. 3 for Lake Michigan test at location of buoy 45007 at October 7, 06z.

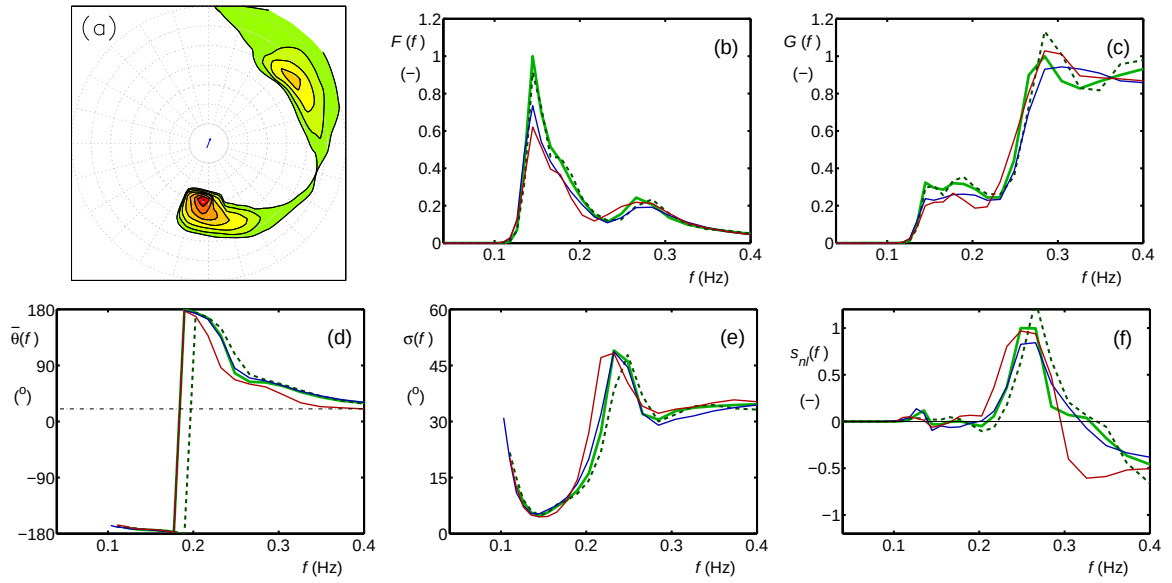

Fig. 9 : Like Fig. 3 for Lake Michigan test at location of buoy 45007 at October 8, 00z.

For the significant wave heights presented in Fig. 7a, the traditional WAM and G11d configurations (dotted and solid red lines) show a small but systematic underestimation of the expected WRT solution (green line). All other configurations, however, including the WW3 configurations (G11d, red line), show excellent results. Similar results are found for the spectral peak frequency (Fig. 7b), where particularly the WW3 configuration overestimates the peak frequency. By now, this is a well established spurious feature of the default WAVEWATCH III model, which can be attributed to its DIA configuration. The mean directions (Fig. 7c) are generally well described, and the directional spread (Fig. 7d) tend to be overestimated by the DIA configurations as expected. Note, however, that the directional spread is not overestimated by the DIA configurations during the peak of the storm event (between hours 24 and 36). Hence, these typical DIA-induced errors cannot always be expected.

Figures 8 and 9 show spectral parameters at the buoy location at the peak of the storm, and at the end of the computation. At the peak of the storm (Fig. 8), the spectrum is dominated by a wind sea with some shearing and separation at low frequencies. All spectral parameters behave as expected for wind seas, with errors of the different interaction parameterizations in line with those expected from the idealized test cases. At the end of the computation, a swell and a wind sea coexist, as is clear in the spectra presented in Fig. 9a-c. Even in these more complex conditions than those used in optimizing the GMD, it is clear that the more complex configurations outperform the traditional DIA configuration. Particularly the swell representation in the spectrum and in the steepness spectrum from the G35d configuration is excellent.

4 DISCUSSION

The results of the hurricane and Lake Michigan tests presented in the previous two sections show a significant improvement of the wave model with increasing complexity of the interaction approximation. Objective error measures, as defined in Tolman (2010b) are presented in Table 2. Errors for the non-optimized configurations (WAM, WW3) are virtually identical to those found in the idealized test. The optimized configurations show a similar pattern of reduction of errors, albeit with a somewhat larger resulting error. The latter could be expected for independent versus dependent tests, whereas the former clearly indicates that the optimization for idealized cases indeed improves practical model behavior, and hence validates the optimization approach used for the GMD.

Table 2: Synopsis of model performance for practical test cases for model configurations of Table 1. T_n is the model run time, normalized with the results of the default wave model with the traditional DIA implementation, ϵ is the objective model error from Tolman (2010b).

	Hurricane		L. Michigan	
ID	T_n (-)	ϵ (%)	T_n (-)	ϵ (%)
WW3	1.20	27.5	1.16	23.5
WAM	0.99	28.7	1.09	24.9
G11d	1.05	26.3	1.10	21.8
G13d	1.50	19.1	1.45	16.8
G35d	3.53	14.9	4.04	14.1
WRT	1360	—	370	—

Table 2 also present normalized run times of the various model configurations, obtained on NCEP's IBM SP using 64 processors[4]. The run times are normalized with the run times of a model with the default DIA implementation in WW3 configuration. The fact that the normalized WW3 run times are larger than 1 by approximately 20% reflects the additional complexity of the shallow water implementation of the GMD and the corresponding increase in computational costs. The WAM and G11d configurations use an GMD configuration with identical computational cost as the WW3 configuration, yet result in somewhat cheaper models. This is associated with the dynamic time stepping scheme for source term integration as used in the wave model; WAM and G11d result in smoother model integration with larger time steps, and hence in a more economical wave model.

The G13d configuration results in a significantly more accurate wave model (see previous sections), at a most increase in run time of approximately 50% (see Table 2). This appears highly feasible in operational wind wave models, and is likely to be introduced in the operational wind wave models at NCEP in the near future.

The most accurate GMD configuration (G35d) re-

[4] More resources were used for the WRT runs, making the corresponding normalized run times estimates.

sults in a more substantial increase of computational costs of typically a factor of 4. This is more difficult to justify in operational wave models, but may become feasible in the near future with the ever increasing power of super computers. This configuration may be a candidate for combination with a Neural Network to accelerate the computations (see Tolman and Krasnopolsky, 2004; Tolman, 2009a). Furthermore, G35d is orders of magnitude more economical that the WRT based computations. Considering its high accuracy, such a configuration should be for research in realistic conditions, where the factor of four increase in run time compared to the traditional DIA should be less of an issue, but where an additional factor of 100-400 (Table 2) for a computation using the WRT methods still is not feasible.

In the introduction, it has been mentioned that the GMD configurations are used as proxies for other methods like SRIAM, that are not (yet) available in WAVEWATCH III. The same is true for other 'exact' approaches and reduced versions thereof. When implemented in WAVEWATCH III, the optimization package for the GMD can be used to objectively benchmark accuracy as well as economy of each approach. Note that the package can use arbitrary model runs as benchmarks, and is not hardwired to the WRT method. It can therefore also be used to intercompare 'exact' approaches, and/or develop or validated GMD configurations against other 'exact' approaches.

5 CONCLUSIONS

A set of Generalized Multiple DIA (GMD) configurations with increasing complexity is used to test the impact of corresponding errors and model improvements in realistic conditions (a synthetic hurricane and a storm on Lake Michigan). It is shown that the traditional DIA results in surprisingly large wave height errors in hurricane conditions, and smaller errors in the Lake Michigan case. In both cases, the DIA results in significant errors in spectral parameters. A GMD with three DIA-style representative quadruplets significantly reduces all errors, at a moderate increase in model run time of approximately 50%. Such an improvement appears feasible and justifiable in operational wave models. A more complex GMD configuration removes most errors at the cost of increasing model run times by a factor 4. This may or may not be feasible for operational wave models, but should be used for research modes as it reduces model run times compared to using the full WRT method by orders of magnitude. The objective accuracy and cost estimates used here can easily be applied to any interaction approximation implemented in WAVEWATCH III.

References

Booij, N., R. C. Ris and L. H. Holthuijsen, 1999: A third-generation wave model for coastal regions, Part I, model description and validation. *J. Geophys. Res.*, **104**, 7649–7666.

Hasselmann, K., T. P. Barnett, E. Bouws, H. Carlson, D. E. Cartwright, K. Enke, J. A. Ewing, H. Gienapp, D. E. Hasselmann, P. Kruseman, A. Meerburg, P. Müller, D. J. Olbers, K. Richter, W. Sell and H. Walden, 1973: Measurements of wind-wave growth and swell decay during the Joint North Sea Wave Project (JONSWAP). *Ergänzungsheft zur Deutschen Hydrographischen Zeitschrift, Reihe A(8)*, **12**, 95 pp.

Hasselmann, S., K. Hasselmann, J. H. Allender and T. P. Barnett, 1985: Computations and parameterizations of the nonlinear energy transfer in a gravity-wave spectrum, Part II: parameterizations of the nonlinear energy transfer for application in wave models. *J. Phys. Oceanogr.*, **15**, 1378–1391.

Komatsu, K., 1996: Development of a new generation wave forecast model based on a new schema of nonlinear energy transfer among wind waves (in Japanese). Ph.D. thesis, Kyoto University, 155 pp.

Komen, G. J., L. Cavaleri, M. Donelan, K. Hasselmann, S. Hasselmann and P. A. E. M. Janssen, 1994: *Dynamics and modelling of ocean waves.* Cambridge University Press, 532 pp.

Masuda, A., 1980: Nonlinear energy transfer between wind waves. *J. Phys. Oceanogr.*, **10**, 2082–2093.

Perrie, W. and D. T. Resio, 2009: A two-scale approximation for efficient representation of nonlinear energy transfer in a wind wave spectrum. Part II: Application to observed wave spectra. *J. Phys. Oceanogr.*, **39**, 2451–2476.

Phillips, O. M., 1981: Wave interaction: the evolution of an idea. *J. Fluid Mech.*, **106**, 215–227.

Resio, D. T. and W. Perrie, 1991: A numerical study of nonlinear energy fluxes due to wave-wave interactions. Part 1: Methodology and basic results. *J. Fluid Mech.*, **223**, 603–629.

Resio, D. T. and W. Perrie, 2008: A two-scale approximation for efficient representation of nonlinear energy transfer in a wind wave spectrum. Part I: Theoretical development. *J. Phys. Oceanogr.*, **38**, 2801–2816.

Tamura, H., T. Waseda, Y. Miyazawa and K. Komatsu, 2008: Current-induced modulation of the ocean wave spectrum and the role of nonlinear energy transfer. *J. Phys. Oceanogr.*, **38**, 2662–2684.

Tolman, H. L., 1991: A third-generation model for wind waves on slowly varying, unsteady and inhomogeneous depths and currents. *J. Phys. Oceanogr.*, **21**, 782–797.

Tolman, H. L., 2009a: Practical nonlinear interaction algorithms. in *11^{th} international workshop on wave hindcasting and forecasting & coastal hazards symposium, JCOMM Tech. Rep. 52, WMO/TD-No. 1533*. Paper J2.

Tolman, H. L., 2009b: User manual and system documentation of WAVEWATCH III ^{TM} version 3.14. Tech. Note 276, NOAA/NWS/NCEP/MMAB, 194 pp. + Appendices.

Tolman, H. L., 2010a: A genetic optimization package for the Generalized Multiple DIA in WAVEWATCH III ®. Tech. Note 289, Ver. 1.0, NOAA/NWS/NCEP/MMAB, 21 pp.

Tolman, H. L., 2010b: Optimum Discrete Interaction Approximations for wind waves. Part 4: Parameter optimization. Tech. Note 288, NOAA/NWS/NCEP/MMAB, 175 pp.

Tolman, H. L., J. H. G. M. Alves and Y. Y. Chao, 2005: Operational forecasting of wind-generated waves by hurricane Isabel at NCEP. *Wea. Forecasting*, **20**, 544–557.

Tolman, H. L., B. Balasubramaniyan, L. D. Burroughs, D. V. Chalikov, Y. Y. Chao, H. S. Chen and V. M. Gerald, 2002: Development and implementation of wind generated ocean surface wave models at NCEP. *Wea. Forecasting*, **17**, 311–333.

Tolman, H. L. and V. M. Krasnopolsky, 2004: Nonlinear interactions in practical wind wave models. in *8^{th} international workshop on wave hindcasting and forecasting, JCOMM Tech. Rep. 29, WMO/TD-No. 1319*. Paper E1.

Tracy, B. and D. T. Resio, 1982: Theory and calculation of the nonlinear energy transfer between sea waves in deep water. WES Report 11, US Army Corps of Engineers.

Van Vledder, G. Ph., 2002: A subroutine version of the Webb/Resio/Tracy method for the computation of nonlinear quadruplet interactions in a wind-wave spectrum. Report 151b, Alkyon, The Netherlands.

Van Vledder, G. Ph., 2006: The WRT method for the computation of non-linear four wave interactions in discrete spectral wave models. *Coastal Eng.*, **53**, 223–242.

WAMDIG, 1988: The WAM model – a third generation ocean wave prediction model. *J. Phys. Oceanogr.*, **18**, 1775–1810.

Webb, D. J., 1978: Non-linear transfers between sea waves. *Deep-Sea Res.*, **25**, 279–298.

WISE Group, 2007: Wave modelling - the state of the art. *Progress in Oceanography*, **75**, 603–674.

Young, I. R. and G. Ph. Van Vledder, 1993: A review of the central role of nonlinear interactions in wind-wave evolution. *Trans. Roy. Soc. London*, **342**, 505–524.